Chapter 2

MIMO-OFDM Baseband Transceiver Architecture

Chapter 2 focuses on the baseband transceiver architecture. An overview of the MIMO-OFDM system will first be given. Then we divide the developed architecture into transmitter and receiver, and provide functional descriptions for each block. Then, the MIMO techniques adopted on the system will be provided. At last, we will include the concept of condition number to identify a MIMO channel, and present the adaptive technique for mode selection among different space-time techniques.

2.1 Introduction of MIMO-OFDM System

OFDM has become a popular technique for transmission of signals over wireless channels. It converts a frequency-selective channel into a parallel collection of frequency flat subchannels, which makes the receiver simpler. The time domain waveforms of the subcarriers are orthogonal, yet the signal spectrum corresponding to the different subcarriers overlap in frequency domain. Therefore, the available bandwidth is used very efficiently, especially compared with those systems having intercarrier guard bands, as shown in Figure 2.1 [6]. In order to eliminate inter-symbol interference (ISI) almost completely, a guard time is introduced for each OFDM symbol. Moreover, to eliminate inter-carrier interference (ICI), the OFDM symbol is further cyclically extended in the guard time, resulting in the cyclic prefix (CP). With proper coding and interleaving across frequencies, multipath turns into an advantage of OFDM system, by yielding frequency diversity. By using Fast Fourier Transform (FFT) at the transmitter and the receiver, OFDM can be implemented efficiently. At the receiver, FFT reduces the channel response into a constant scalar on each subcarrier. With MIMO, the channel response becomes the form of a matrix. Since each subcarrier can be equalized independently, the complexity can be reduced significantly. Multipath remains an advantage for a MIMO-OFDM system since the frequency selectivity caused by multipaths can improve the rank distribution of the channel matrices across those subcarriers, thereby increasing system capacity. We summarize the advantages of OFDM as follows [1]:

1. High spectral efficiency
2. Simple implementation by FFT
3. Robustness against narrowband interference
4. High flexibility in terms of link adaptation for having many subcarriers.
5. Suitability for high-data-rate transmission over a multipath fading channel

Multiple antennas can be used at the transmitter and the receiver, now widely termed a MIMO system. A MIMO system exploits the spatial diversity obtained by spatially separated antennas especially in a dense multipath scattering environment. There are a number of different ways to obtain either a diversity gain to combat signal fading or to obtain a capacity gain to increase throughput, which we will give a more detailed explanation in the following two subsections. Therefore, after OFDM is combined with MIMO techniques, MIMO-OFDM can be a potential candidate for the next generation wireless communication systems.

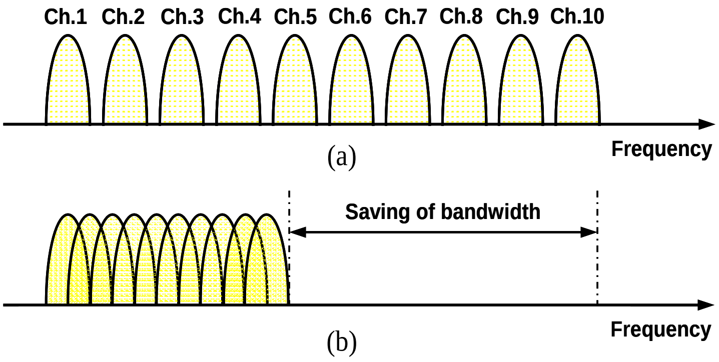

Figure 2.1: (a) Conventional multicarrier technique

(b) Orthogonal multicarrier modulation technique

2.2 Transmitter Architecture

Figure 2.2 shows a block diagram of a MIMO-OFDM transmitter. The source data is first fed into the channel encoder, e.g., using the convolutional code for error correction at the receiver. The encoded output is then interleaved by distributing the same coded bits into different positions in the packet so that the transmitted information is more resistant to the channel distortion. A MIMO system is typically designed to meet two different, yet opposite, targets: either to achieve high spectral efficiency, e.g., the V-BLAST scheme suggested by Foschini *et al.* [3], or to improve the transmission reliability against channel fading, e.g., the STBC [2] first discovered by Alamouti for two transmit antennas. To simultaneously acquire the efficiency and reliability advantages, we can adopt a flexible transmission mechanism, which can switch between V-BLAST and STBC, and also allows for a joint operation called G-STBC [4][5]. The flexibility of the proposed "triple-mode" MIMO transmitter can balance the bit error rate and throughput and obtain an overall optimal utilization of resources. The preamble channels, including short preamble coded by rule of STBC and long preamble without coded, will be attached in front of data channel modulated by the inverse FFT (IFFT). Finally, all traffic data composed of preamble part and data channels are filtered by the RRC filter and sent to individual channels of digital to analog (D/A) modules to convert the baseband digital signals to analog signals. In the following subsections, we will choose some important functional blocks to give a detailed description.

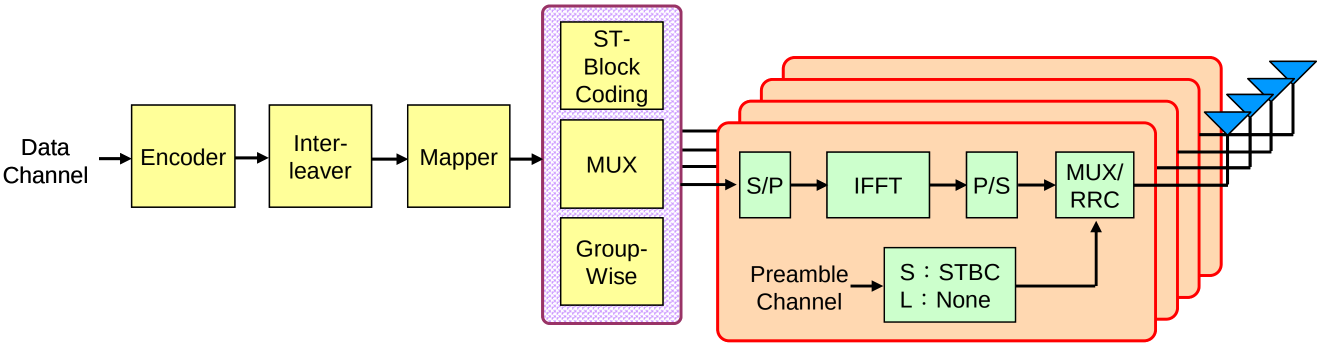

Figure 2.2: Transmitter architecture of the adaptive 4×4 MIMO-OFDM system

2.2.1 Convolutional Encoder

A convolutional code maps each k bits of a continuous input stream on n output bits, where the mapping is performed by convolving the input bits with a binary impulse response. In general, it can be implemented simply by shift registers and modulo-2 adders. Figure 2.3 shows a convolutional encoder [7]-[9] implemented in our system with $k=1$, $n=3$, and code rate$=k/n=1/3$. This encoder has a single data input and three outputs A_i, B_i, and C_i, which are interleaved to form the coded output sequence $\{A_1B_1C_1A_2B_2C_2\ldots\}$.

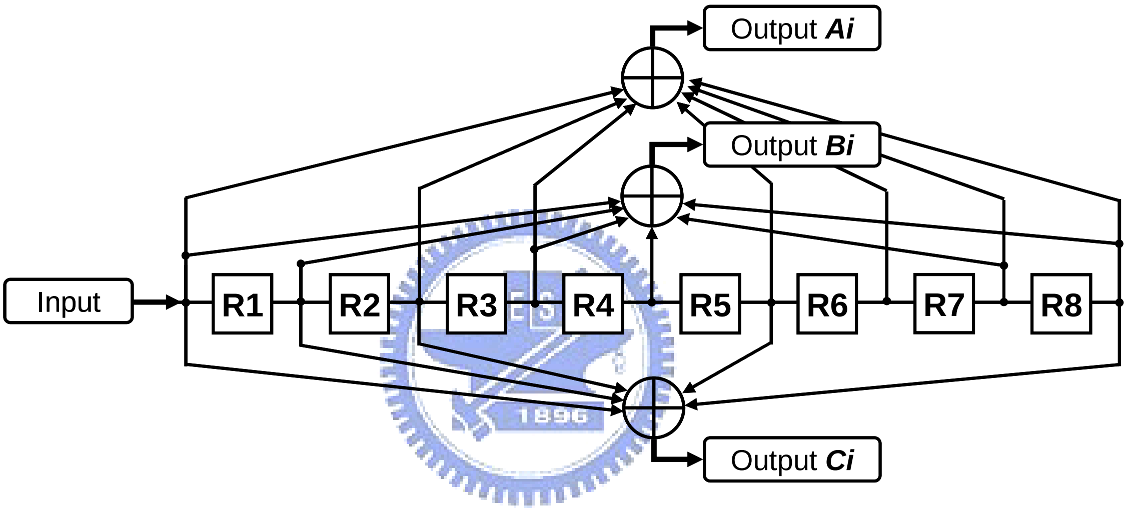

Figure 2.3: Convolutional encoder with code rate1/3

2.2.2 Interleaver / De-interleaver

Because of the frequency selective fading of typical radio channels, the OFDM subcarriers generally have different amplitudes. Deep fades in frequency spectrum may cause groups of subcarrier to be less reliable than others, which cause bit errors in bursts rather than being scattered randomly. Most forward error-correction codes are not designed to deal with burst errors, while an interleaver is applied to randomize the occurrence of bit errors prior to decoding, and thereby, is able to combat with burst errors. At the transmitter, the coded bits are permuted in a certain way so that adjacent bits are separated by several bits after interleaving. At the receiver, the reverse permutation is performed before decoding. A commonly used interleaving scheme is the block interleaving, where the input bits are written in a matrix column by column and read out row by row.

Referring to institute of electrical and electronics engineers (IEEE) 802.11a standard [10], we use a block interleaver as shown in Figure 2.4. In the standard, the interleaving depth is suggested being the length of an OFDM symbol. Each coded data symbol after convolutional encoder contains 96 bits. Therefore the interleaving depth we adopt is 96, as illustrated in the above figure. The interleaver satisfies the following expression

$$j = 6 \times (k \bmod 16) + \lfloor k / 16 \rfloor$$

where k is the index of input coded data, and $k = 0,1,\ldots,95$; j is the index of output interleaved data; $\lfloor m \rfloor$ is the greatest integer smaller than m. The figure shows the bit numbers of a block interleaving operating on a block size of 96 bits. At the transmitter, the interleaver follows the direction indicated by solid arrows. After writing the 96 bits in the matrix according to the order as depicted in the figure, the interleaved bits are read out column by column. At the receiver, the de-interleaver performs opposite to the transmitter and follows the direction of the dotted arrows.

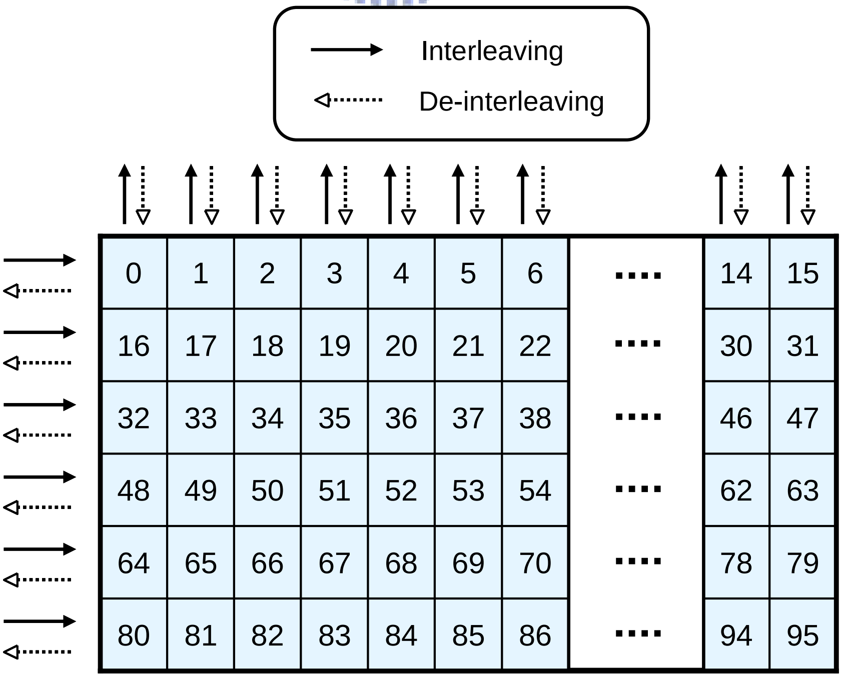

0	1	2	3	4	5	6	....	14	15
16	17	18	19	20	21	22	....	30	31
32	33	34	35	36	37	38	....	46	47
48	49	50	51	52	53	54	....	62	63
64	65	66	67	68	69	70	....	78	79
80	81	82	83	84	85	86	....	94	95

Figure 2.4: Interleaver and de-interleaver schemes

2.2.3 Mapper / De-mapper

Quadrature amplitude modulation (QAM) is the most popular type of modulation using in the OFDM system. The rectangular constellations are especially easy to implement as they can be split into independent in-phase and quadrature parts. A mapper is used to map a small group of bits into a symbol according to the rectangular constellation adopted. Figure 2.5 shows the rectangular constellations of Quadrature Phase Shift Keying (QPSK), 16-QAM, and 64 QAM. The higher modulation order the mapper adopts, the more information a symbol can carry, yet higher modulation order always suffers from interference more severely. In our system, we only adopt QPSK as our modulation scheme.

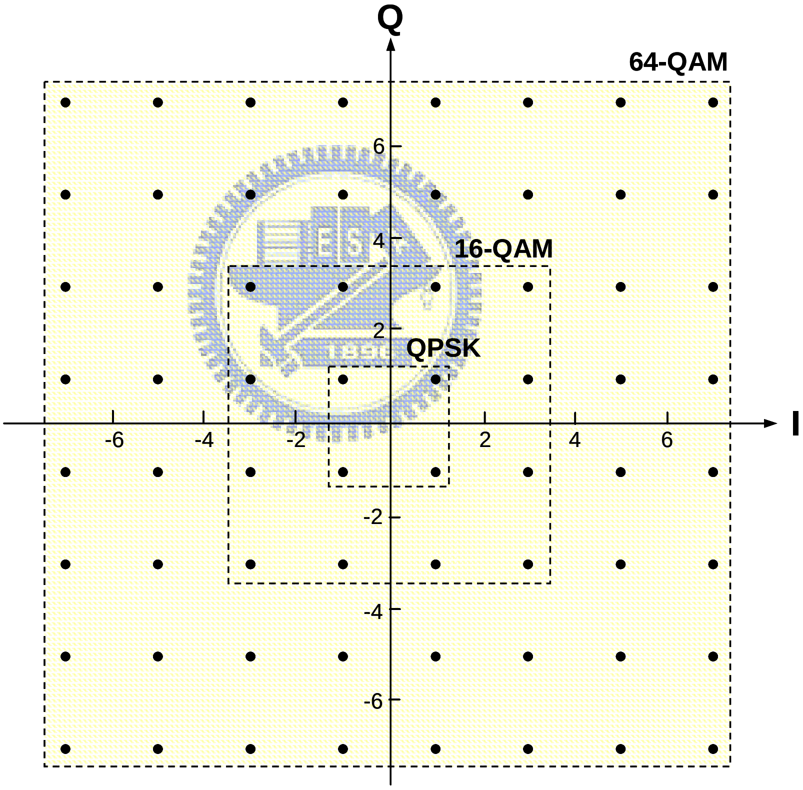

Figure 2.5: QPSK, 16-QAM, and 64-QAM constellations

2.2.4 Preamble Channel and Frame Structure

Referring IEEE 802.11a standard [10], we attach the training sequence, also called preamble, in front of every packet. At the receiver, preambles can be utilized to do a number of tasks, such as timing synchronization, frequency synchronization, and channel estimation. The format of preamble channel and frame structure is shown in Figure 2.6 [10]. Preambles can further be separated into sort preambles and long preambles. Short preambles, as implied by the name, have a shorter length compared with long preambles. Each short preamble symbol contains 16 bits with time-span 0.8 μs, and ten symbols form a complete short preamble with a total time-span of 8 μs. In the proposed system, short preambles are mainly used for timing synchronization. The following parts are two long preambles, and each one is protected by a guard interval filled with its cyclic extension, which have a total time-span of 8 μs. After preamble channels, data symbols with cyclic extension follow. Note that the first non-preamble symbol is designed for signaling in the standard, such as code rate and modulation order. In our implementation, we adopt four long preamble symbols for channel estimation transmitted in different antennas with different time delays, and we will give a more detailed introduction with the topic called preamble design in chapter 4.

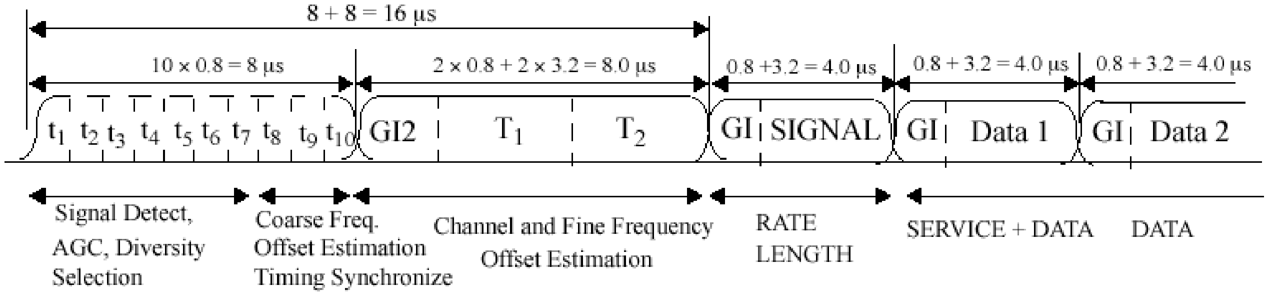
8 + 8 = 16 μs
10 × 0.8 = 8 μs
2 × 0.8 + 2 × 3.2 = 8.0 μs
0.8 +3.2 = 4.0 μs
0.8 + 3.2 = 4.0 μs
0.8 + 3.2 = 4.0 μs
t1 t2 t3 t4 t5 t6 t7 t8 t9 t10
GI2
T1
T2
GI
SIGNAL
GI
Data 1
GI
Data 2
Signal Detect, AGC, Diversity Selection
Coarse Freq. Offset Estimation Timing Synchronize
Channel and Fine Frequency Offset Estimation
RATE LENGTH
SERVICE + DATA
DATA

Figure 2.6: Training sequence and frame structure of IEEE 802.11a standard

2.3 Receiver Architecture

The baseband functional diagram of the proposed MIMO-OFDM receiver is shown in Figure 2.7. The received signal is first converted to digital signals in the baseband. After passing through RRC, data streams are processed by FFT. To acquire the timing information, short preamble is used to make initial estimates of the frame start. Then long preamble is added to do a finer estimation. In a high signal to noise ratio (SNR) situation, a coarse estimate can just suffice. To compensate the frequency offset, we use the idea that nearby data suffer ascending frequency offset and can be gathered to obtain an associated estimate. We will also include pilot subcarriers inserted in data channel to estimate the phase shift in a packet to further improve the performance. The training pattern is sent using an identity structure matrix and, by exploiting the structure of orthogonality, such that the estimation of channel state information (CSI) can be done in frequency domain. After FFT processing and some corrections, data are passed into the space-time detector used for separating the multi-antenna signals. The detected symbol streams are then de-interleaved, followed by a Viterbi decoder to recover the source bits. Since the transmitted signals can be space-time block encoded, spatially multiplexed, or a mixed version of both, the space-time detector has to perform the corresponding decoding scheme according to the space-time processing scheme adopted in the transmitter. In the following subsections, we will discuss some important functional blocks in detail.

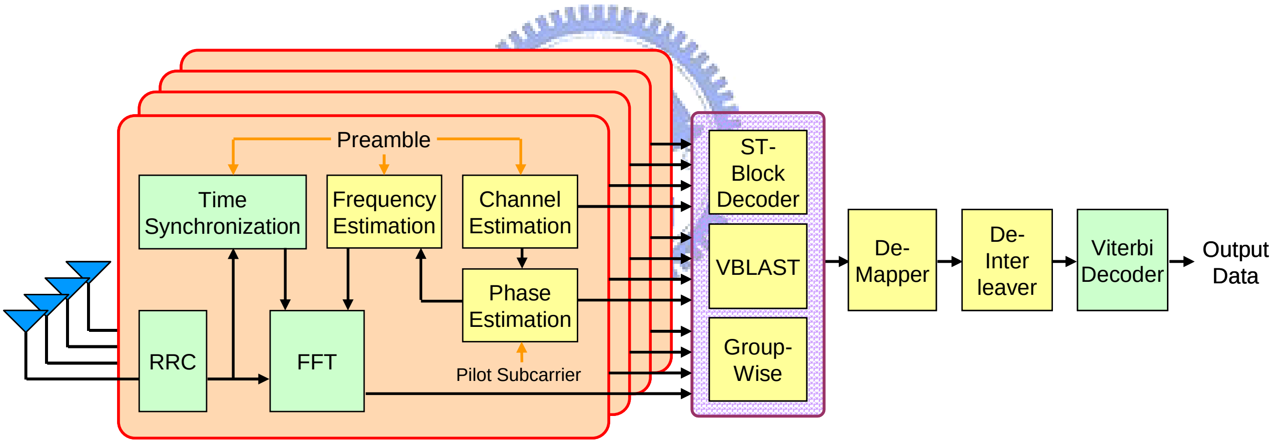

Figure 2.7: Receiver architecture of an adaptive 4×4 MIMO-OFDM system

2.3.1 Synchronization

Before an OFDM receiver can demodulate the subcarriers, it has to perform at least two synchronization tasks. First, it has to find out where the symbol boundaries are and what the optimal timing instants are to minimize the effects of ICI and ISI. Second, it has to estimate and correct for the carrier frequency offset of the received signal, because any offset introduces ICI. In fact, these two synchronization tasks are not the only training required in an OFDM receiver. For coherent receivers, except for the frequency, the carrier phase also needs to be synchronized. In the proposed system, timing synchronization can be further divided into coarse timing synchronization and fine timing synchronization [11][12]. In the flowing subsections, we will discuss coarse timing, fine timing, frequency synchronization techniques and phase tracking technique.

2.3.1.1 Coarse Timing Synchronization

The main task of the coarse timing synchronization is frame detection, which is to identify the preamble in order to detect a packet arrival. In our implementation, the short preamble is used to perform the coarse timing algorithm based on the correlation between the repeated symbols constituting the preamble.

In the coarse timing synchronization stage, a matched filter (MF) with the length of ten short preamble (SP) symbols is used. After passing through the MF, we can obtain the output $y_1(n)$ and $y_1(n+1)$ as follows:

$$y_1(n) = (s^{(1)}(n)h_1^{(1)} + s^{(2)}(n)h_1^{(2)}) \cdot e^{j2\pi\Delta_f nT_b}$$

$$y_1(n+1) = (-s^{(2)*}(n)h_1^{(1)} + s^{(1)*}(n)h_1^{(2)}) \cdot e^{j2\pi\Delta_f (n+1)T_b}$$

Square and sum up the above two equations, we can obtain

$$\begin{aligned} w_1(n) &= \left|y_1(n)\right|^2 + \left|y_1(n+1)\right|^2 \\ &= \left(\left|s^{(1)}(n)\right|^2 + \left|s^{(2)}(n)\right|^2\right)\left(\left|h_1^{(1)}(n)\right|^2 + \left|h_1^{(2)}(n)\right|^2\right) \end{aligned}$$

Then we find $\hat{\tau}_{\text{init}}$ that can maximize the summation of all SPs and received antennas.

$$x_1(n) = \sum_{m=0}^{8} w_1(n+m) + \text{other antennas}$$

$$\hat{\tau}_{\text{init}} = \arg \max_{n} \left\{x_1(n), x_2(n), \ldots, x_{16}(n)\right\}$$

where $\hat{\tau}_{\text{init}}$ is the start timing of a frame. Owing to the STBC structure applied to two adjacent SP symbols, some diversity can be obtained. After MF, nine peak values can be obtained since ten SP symbols are transmitted, and each time-span between two peaks has a length of 16, which is also the period of a SP symbol. To acquire a more accurate frame position, data after MF is further passed to a finite impulse response (FIR) filter so that we can obtain a succession of increasing peaks and finally choose the time instant a deterministic delay away from the maximum value as the frame start.

2.3.1.2 Fine Timing Synchronization

The symbol timing in an OFDM system decides where to place the start of the FFT window within the OFDM symbol. Although an OFDM system exhibits a guard interval, making it somewhat robust against timing offsets, non-optimal symbol timing will cause more ISI and ICI in delay spread environments. This will result in performance degradation. To eliminate timing offset induced by different path delays, fine timing synchronization will be performed after coarse timing synchronization.

As illustrated in Figure 2.8, an MF using four successive long preambles as its coefficients is applied to do window integral over the range of seven samples before and after the coarse timing estimate and the results are accumulated over four long preambles. Then we choose the timing offset that has the maximum integral and dump value to be the new fine-synchronized timing.

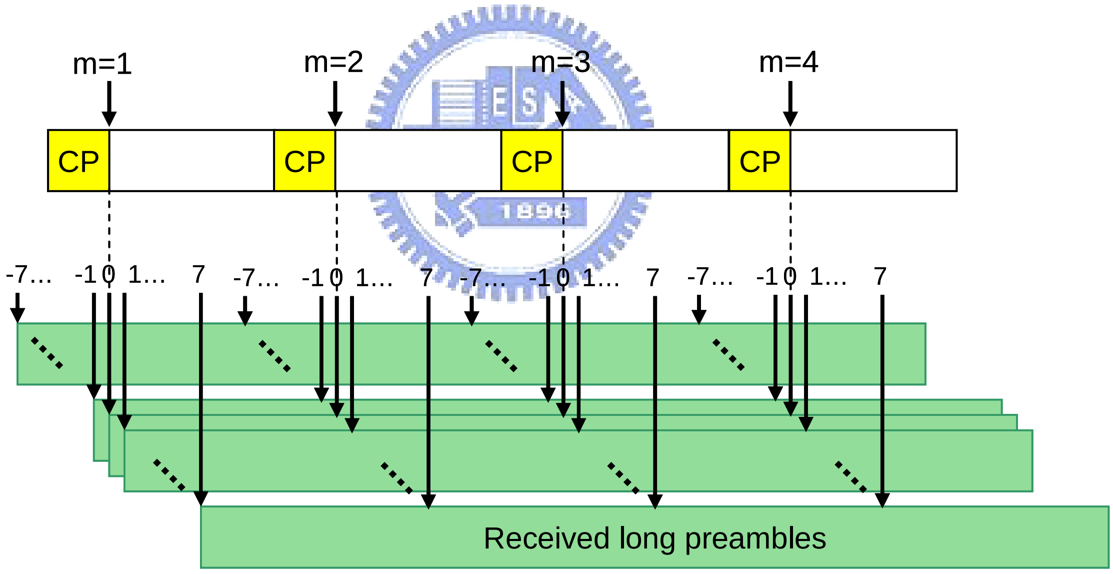

Figure 2.8: Fine timing synchronization scheme

2.3.1.3 Frequency Synchronization

The purpose of frequency synchronization is to correct the frequency offset, which is caused by the difference of oscillator frequencies at the transmitter and the receiver. Frequency offset may result in the loss of the orthogonality between subcarriers and degrade the system performance. Therefore, we try to estimate the frequency offset and compensate the received signals.

In this thesis, we use pilot tones inserted at some specific subcarriers to calculate the phase shift in a packet. Sending real-valued pilot tones at the transmitter, we expect to receive the real-valued pilot signals if there is no channel interference and frequency offset. After adding the effect of estimated channel on original pilot data and then taking a complex conjugation, we can multiply them with the received pilot data. Then, at each adjacent sample pairs we perform correlation computations to find out the phase drift between samples. The diagram of the concept is illustrated in Figure 2.9. If the number of symbols in a packet is n, then we have $n-1$ adjacent correlation pairs. Since we have four pilot tones forming $4(n-1)$ adjacent pairs, phase rotation between two adjacent pilot data can be obtained by taking an average over those correlations. Hence, the frequency offset can be found by simply dividing the averaged phase shift by $2\pi T$.

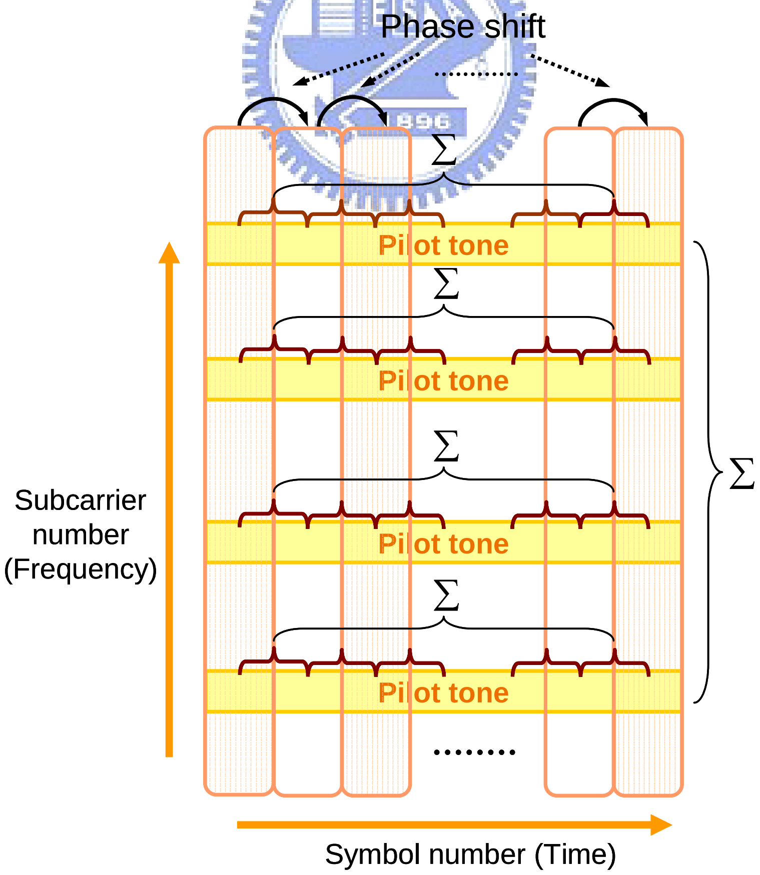

Figure 2.9: Frequency synchronization concept

2.3.1.4 Phase Tracker

Phase tracking can be regarded as a remedy after over-compensating the signals by estimated frequency offset mentioned in Section 2.3.1.3 because there always exists a difference between the estimated one and actual one. Since the estimated frequency offset is derived from the average phase shift among all symbols, it apparently cannot be suitable for all the samples, especially those on different symbols. Therefore, phase tracker is needed to correct the over-compensated signals. Compared with frequency offset estimation, instead of doing correlation between adjacent samples and averaging all the symbols, the scheme used by the phase tracker only averages the phase residue among four pilot tones in each symbol. Therefore, we may have the information for phase tracking on a symbol-by-symbol basis.

2.3.2 Channel Estimator

Long preambles are used to carry out the major task of channel estimation. Owing to the same symbol structure as data symbols, long preamble becomes the best candidate for performing this job. A receiver can perform the channel estimation by taking FFT of the averaged received long training symbols and do a vector-wised comparison. As shown in Figure 2.10, after taking FFT of received long training symbols, we also need to transform the original long training symbols into frequency domain. Thus, the channel frequency response can be obtained simply by dividing the FFT output of received training symbols and the FFT output of the original training symbols.

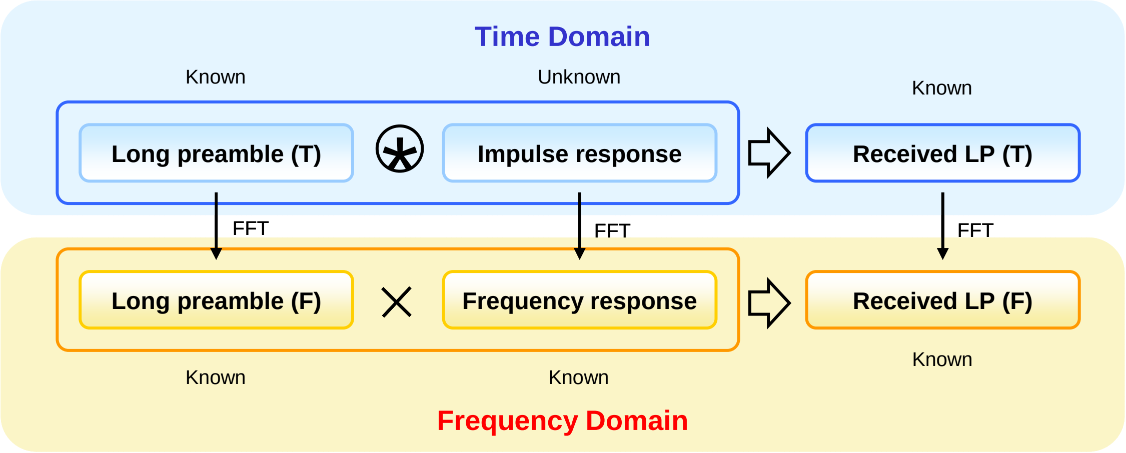

Figure 2.10: Channel estimation scheme

2.3.3 Viterbi Decoder

Decoding of convolutional codes is most often performed by the soft decision Viterbi decoder, which is an efficient way to obtain the optimal maximum likelihood estimate of the encoded sequence. The complexity of Viterbi decoding grows exponentially with the constrain length. In our implementation, the constraint length is 9, and the number of states is 256 [13].

2.4 MIMO Techniques

The use of MIMO antenna systems leads to dramatic improvements in capacity and link reliability of wireless systems. Current space-time processing techniques [14]-[16] for MIMO system typically fall into two categories, data rate maximization and diversity maximization schemes, though there has been some effort toward the joint scheme recently. In this thesis, we mainly consider MIMO techniques in three modes, MIMO diversity, spatial multiplexing, and a hybrid scheme called G-STBC, which we will give a more detailed discussion in the following subsections.

2.4.1 MIMO Diversity

In wireless communication systems, diversity techniques are widely used to reduce the effects of multipath fading and improve the reliability of transmission without increasing the transmitted power or sacrificing the bandwidth. Diversity techniques are classified into time, frequency, and space diversity. Space diversity, also called antenna diversity, can be further classified into two categories, transmit diversity and receive diversity. Among various transmit diversity schemes, STBC is the most popular scheme with the feature of open loop (i.e., no feedback signaling is required) as channel information is not needed at the transmitter. Therefore we will focus on the scheme of STBC in this section.

The space-time block coding scheme was first discovered by Alamouti [2] (hence the name Alamouti’s code) for two transmit antennas. Symbols transmitted from those antennas are encoded in both space and time in a simple manner to ensure that transmissions from both the antennas are orthogonal to each other. This would allow the receiver to decode the transmitted information with a slight increment in the computational complexity. In the following discussion, we will first give an overview of Alamouti's scheme, and then extend to the case of STBC with more transmit antennas.

Alamouti's Scheme (with Two Transmit Antennas)

The input symbols to the space-time block encoder are divided into groups of two symbols. At a given symbol period, the encoder takes a block of two modulated symbols c_1 and c_2 in each encoding operation and maps them to the transmit antennas according to a code matrix given by

$$\mathbf{C} = \begin{bmatrix} c_1 & -c_2^* \\ c_2 & c_1^* \end{bmatrix}$$

The encoder outputs are transmitted in two consecutive transmission periods from two transmit antennas. Let h_{11} and h_{12} be the channel gains from the first and second transmit antennas to the only one receiver antenna. Assume that h_{11} and h_{12} are scalar and constant over two consecutive symbol periods. The received signals in two consecutive symbol periods, denoted as r_1 and r_2, can be expressed as

$$\begin{aligned} r_1 &= h_{11}c_1 + h_{12}c_2 + n_1 \\ r_2 &= -h_{11}c_2^* + h_{12}c_1^* + n_2 \end{aligned}$$

where n_1 and n_2 are AWGN noise modeled as identical independent distributed (i.i.d.) complex Gaussian random variables with zero mean and power spectral density $N_0/2$ for each dimension. The above equation can be rewritten in a matrix form as

$$\mathbf{r} = \begin{bmatrix} r_1 \\ r_2^* \end{bmatrix} = \underbrace{\begin{bmatrix} h_{11} & h_{12} \\ \left(h_{12}\right)^* & -\left(h_{11}\right)^* \end{bmatrix}}_{\mathbf{H}} \underbrace{\begin{bmatrix} c_1 \\ c_2 \end{bmatrix}}_{\mathbf{c}} + \underbrace{\begin{bmatrix} n_1 \\ n_2^* \end{bmatrix}}_{\mathbf{n}} = \mathbf{H}\cdot\mathbf{c} + \mathbf{n}$$

Since the channel matrix **H** is unitary, i.e. $\mathbf{H}^H\mathbf{H} = \rho \cdot \mathbf{I}$, where $\rho = \left|h_{11}\right|^2 + \left|h_{12}\right|^2$, the ML decoder can perform an MRC operation on the modified signal vector $\tilde{\mathbf{r}}$ given by

$$\begin{aligned}\tilde{\mathbf{r}} &= \mathbf{H}^{H}\cdot\mathbf{r} = \rho\cdot\mathbf{c} + \underbrace{\mathbf{H}^{H}\cdot\mathbf{n}}_{\tilde{\mathbf{n}}} \\ &= \rho\cdot\mathbf{c} + \tilde{\mathbf{n}}\end{aligned}$$

Therefore, we can obtain the space-time decoded vector $\mathbf{c}$.

STBC with Four Transmit Antennas

Using the theory of orthogonal designs, the simple scheme proposed in [2] was easily generalized to systems with more than two transmit antenna [17]. Before introducing those coding matrix, we first define the rate R of STBC as $R = k/T$ where k is the number of symbols the encoder takes as its input in each encoding operation and T is the number of transmission periods required to transmit the space-time coded symbols through the multiple transmit antennas. The rate of STBC with full transmit diversity must be less than or equal to one, $R \le 1$. The Alamouti scheme is unique in that it is the only space-time block code with an $M_T \times M_T$ complex transmission matrix to achieve the full rate [18]. For an arbitrary complex signal constellation, there are space-time block codes that can achieve a rate of 1/2 for any given number of transmit antennas. The case of four transmit antennas has two rates of coding matrix including 1/2 and 3/4 with complex orthogonal designs, and the later one is adopted in our implementation on account of higher throughput. The coding matrix of STBC with rate 3/4 presented in [19] is depicted in Figure 2.11.

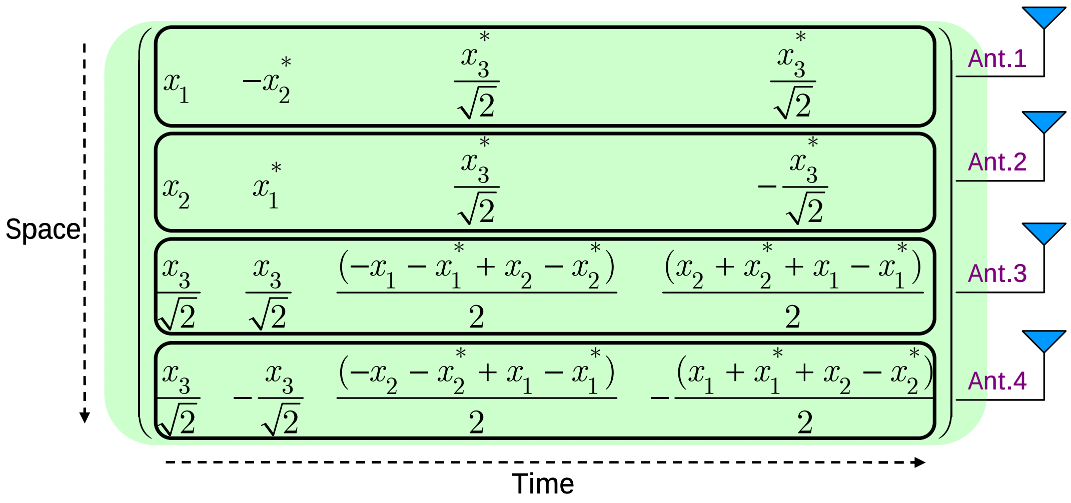

$$\begin{pmatrix} x_1 & -x_2^* & \frac{x_3^*}{\sqrt{2}} & \frac{x_3^*}{\sqrt{2}} \\ x_2 & x_1^* & \frac{x_3^*}{\sqrt{2}} & -\frac{x_3^*}{\sqrt{2}} \\ \frac{x_3}{\sqrt{2}} & \frac{x_3}{\sqrt{2}} & \frac{(-x_1 - x_1^* + x_2 - x_2^*)}{2} & \frac{(x_2 + x_2^* + x_1 - x_1^*)}{2} \\ \frac{x_3}{\sqrt{2}} & -\frac{x_3}{\sqrt{2}} & \frac{(-x_2 - x_2^* + x_1 - x_1^*)}{2} & -\frac{(x_1 + x_1^* + x_2 - x_2^*)}{2} \end{pmatrix}$$

Figure 2.11: STBC coding matrix with rate 3/4

2.4.2 Spatial Multiplexing

Spatial multiplexing technique multiplexes multiple spatial channels to send as many independent data as possible over different antennas for a specific error rate. There are four spatial multiplexing schemes: diagonal BLAST (D-BLAST), horizontal BLAST, V-BLAST, and turbo BLAST [20]. Of them, V-BLAST is the most promising for its implementation simplicity, which will be focused in this section.

In V-BLAST, the encoding process is simply a de-multiplex operation followed by independent substreams. No inter-substream coding, or coding of any kind, is required, though conventional coding of the individual substreams may certainly be applied. Moreover, when compared with D-BLAST, V-BLAST has no lost of triangles in the beginning and the end, and only one-dimension code is required, which leads to a lower complexity. The encoding concept is illustrated in Figure 2.12.

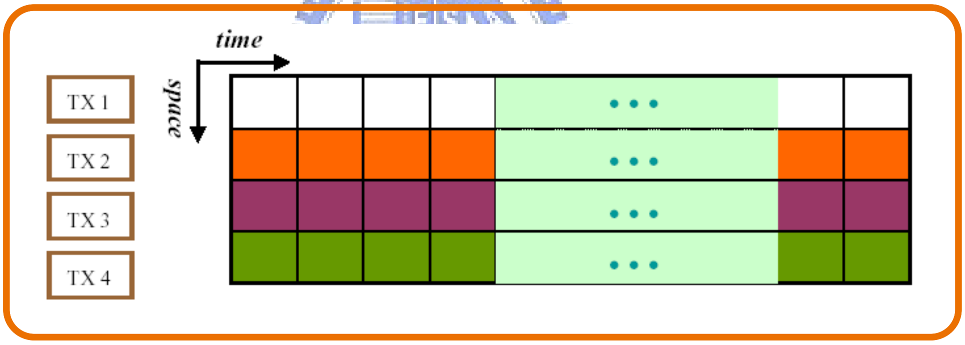

Figure 2.12: V-BLAST encoding procedure

The V-BLAST decoding scheme can simply be performed by computing the interference nulling vectors and de-correlating the received data. Conceptually, each substream in turn is considered to be the desired data, and the remainder are considered as interferences. Nulling is done by linearly weighting the received signals so as to satisfy some performance-related criterion, such as minimum mean-square error (MMSE) or zero-forcing (ZF). It is discovered that superior performance is obtained if nonlinear techniques are used. One particularly attractive nonlinear method is using symbol cancellation as well as linear nulling to perform detection. Using symbol cancellation, interference from already-detected components is subtracted out from the received signal vector, resulting in a modified received vector in which less interferences are present. The concept is somewhat similar to decision feedback equalization, which is illustrated in Figure 2.13. When symbol cancellation is used, the system performance is affected by the order it performs. Therefore, how to decide the process order is important to the overall performance of the system. Here, we only introduce the decoding concept and neglect the detailed mathematical derivations.

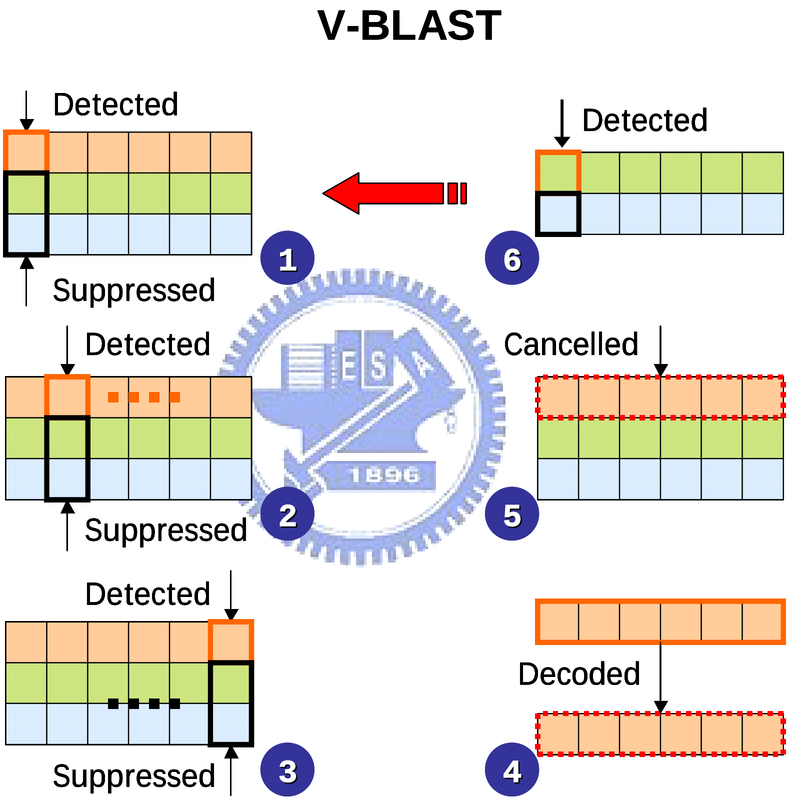

Figure 2.13: V-BLAST decoding procedure

In our implementation, the computational complexity is always our major concern rather than the performance due to the restriction of limited resources in hardware platform. Therefore, we use pure nulling method to perform the decoding at the receiver instead of combining with symbol cancellation which requires higher complexity and more hardware costs.

2.4.3 Group Wise STBC

In a BLAST system, different data streams are transmitted by different transmit antennas, and it is considered the most efficient way to improve the throughput dramatically. However, owing to exploiting the multiplexing gain for throughput, BLAST system always has lower resistance to the same channel condition compared with STBC system, which obtains a diversity gain proportional to the number of transmit antennas. Although BLAST system always performs poorer than STBC system, it can provide a higher transmission rate with a multiple of four in our case. It strongly implies that maybe we need a tradeoff version between BLAST system and STBC system depending on the requirement of throughput or link quality. This is why G-STBC comes out.

G-STBC system can be taken as a hybrid structure of STBC and BLAST MIMO system. In such a system, the transmit antennas are partitioned into several groups. Different data streams are transmitted in each group; therefore the overall transmission data rate will be increased linearly with the number of antenna groups. Within each antenna groups, STBC will be applied and thus the system robustness against fading is improved. The diagram illustrated in Figure 2.14 shows the concept of G-STBC. In our implementation, we divide four transmit antenna into two groups. Different data streams are transmitted via different groups respectively and each group applies Alamouti STBC.

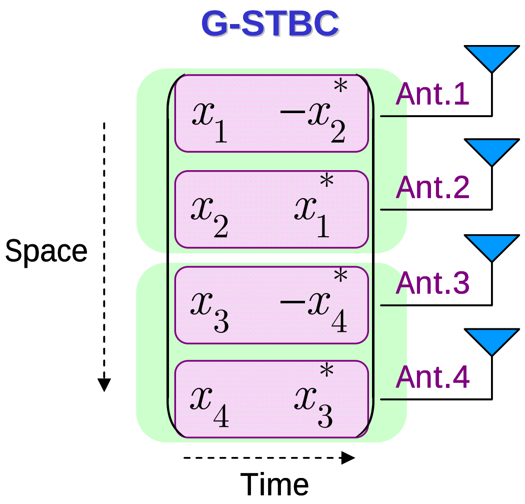

Figure 2.14: G-STBC coding concept

Such a system has been studied in [21] which showed that the minimum number of receive antennas required is equal to the number of transmit antenna groups. Such a structure is very attractive for downlink transmission, with the consideration the miniature size of the mobile terminal, as well as the high data rate requirement at the terminal.

2.5 Adaptive Techniques for Mode Selection

Each space-time algorithm can either perform well or poorly over some specific channel conditions, which implies that there is always no optimal mode for the changing environment. Therefore, in this section, we first try to analysis some classical channels in a view of the degree of correlation, helping us to classify channels according to some characteristics, such as the condition number. Under the categorized channels, we try to give some suggestion for mode selection amount those previously-mentioned space-time algorithms.

2.5.1 MIMO Channels

When spatial processing is employed, the radio frequency channel between transmitter and receiver antenna array elements is commonly referred to as a MIMO channel. In general, the channel response is time dispersive caused by fading effects, implying that the channel response $\mathbf{H}$ varies with frequency. Fading channel results from various environmental objects (buildings, trees, mountains, etc.) which scatter the transmit signals and form either constructive or destructive interference. In our system, the MIMO channel between transmitter and receiver can be represented in matrix form as

$$\mathbf{H}_{\mathbf{R}}(k) = \begin{bmatrix} h_{11}(k) & h_{12}(k) & h_{13}(k) & h_{14}(k) \\ h_{21}(k) & h_{22}(k) & h_{23}(k) & h_{24}(k) \\ h_{31}(k) & h_{32}(k) & h_{33}(k) & h_{34}(k) \\ h_{41}(k) & h_{42}(k) & h_{43}(k) & h_{44}(k) \end{bmatrix}$$

where $h_{ij}(k)$ is the channel response between receiver element i and transmitter element j, and k is the OFDM subcarrier index. $\mathbf{H}_{\mathbf{R}}(k)$ has a dimension of $N_R \times N_T$ where N_R is the number of transmitter antenna elements and N_T is the number of transmitter antenna elements. The order of diversity gain on the MIMO channel is limited by the product of N_R and N_T. When sufficient scattering exists, the maximum number of spatial transmission channels available is bounded by $\min(N_R, N_T)$. Space-time processing permits the system design to trade off between diversity gains and number of spatial streams on a MIMO channel.

Since our system design is highly related to the channel condition, we need to further investigate the MIMO channel. A classification of MIMO fading channels is proposed in [22] and listed as follows:

- Uncorrelated high-rank (UHR, a.k.a., i.i.d.) model: The elements of **H** are i.i.d. $\mathcal{CN}(0,1)$.

- Uncorrelated low-rank (ULR) (or "pinhole") model: $\mathbf{H} = \mathbf{g}_{rx}\mathbf{g}_{tx}^H$, where $\mathbf{g}_{rx}$ and $\mathbf{g}_{tx}$ are independent receive and transmit fading vectors, with $\mathbf{g}_{rx}$ and $\mathbf{g}_{tx}$ being $\mathcal{CN}\left(0,\mathbf{I}_{M_R}\right)$ and $\mathcal{CN}\left(0,\mathbf{I}_{M_T}\right)$ distributions, respectively. It is noteworthy that in this model, rank of every realization of $\mathbf{H}$ is one, and therefore, the ergodic capacity obtained by the spatial diversity technique must be expected to be less than that in the UHR model. This is because there is no multiplexing gain. In this case, the diversity order is equal to $\min(N_R, N_T)$.

- Correlated low-rank (CLR) model: $\mathbf{H} = g_{rx} g_{tx}^* \mathbf{u}_{rx} \mathbf{u}_{tx}^H$, where g_{rx}~$\mathcal{CN}(0,1)$ and g_{tx}~$\mathcal{CN}(0,1)$ are independent random variables, and $\mathbf{u}_{rx}$ and $\mathbf{u}_{tx}$ are fixed deterministic vectors of size $N_R \times 1$ and $N_T \times 1$, respectively, with unit modulus entries. This model yields no diversity or multiplexing gain whatever, just receive array gain.

After giving an overview of channel classification, in the next subsection, we will propose a method to distinguish which kind of channel is experienced at present.

2.5.2 Determination of Channel Condition

Before we determine the channel condition, we first introduce a key channel characteristic that influences the system design, called condition number. The condition number is defined as a ratio of the maximum and minimum eigenvalues of the MIMO channel matrix [23][24]. In our implementation, we only try to distinguish the CLR channel and UHR channel for the sake of simplicity; there exists a much larger difference between them when compared with the CHR channel. Since a CLR channel is a rank deficient channel, the condition number of the channel matrix will be very large. On the other hand, the condition number associated with a UHR channel is moderate due to that a UHR channel is a full rank channel.

An example obtained by a 4×4 MIMO system is used to investigate the relationship between the condition number and the channel types (CLR and UHR channels) [25]. The number of samples is 1000. Figures 2.15 and 2.16 shown the condition numbers of the CLR and UHR channels, respectively, and obviously indicate that the condition number of a CLR channel (minimum value is equal to 2×10^{16}) is much larger than that of the a channel (maximum and mean values are equal to 6×10^{2} and 10.87). Therefore, we can conclude that a CLR channel is determined when the condition number of the channel matrix is larger than10^{3}. Otherwise, the channel is a UHR channel.

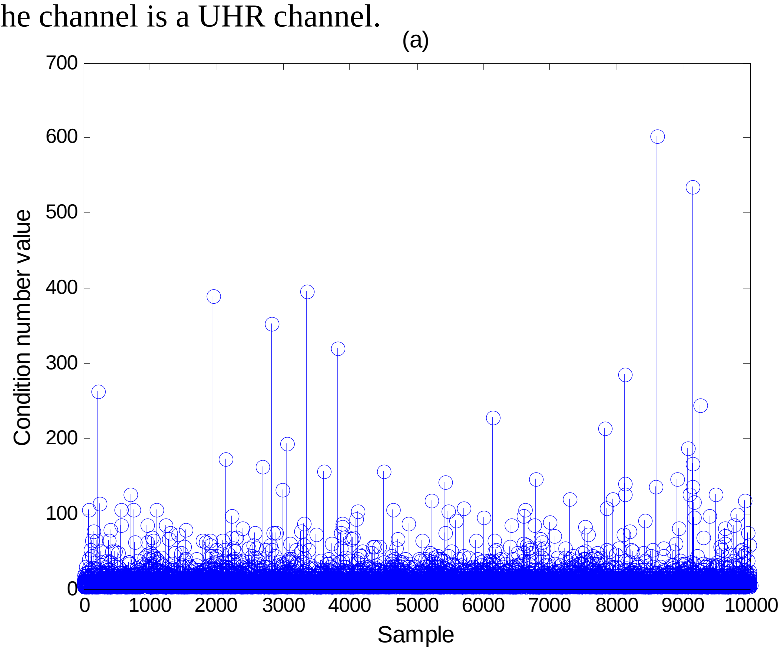

Figure 2.15: Condition number of 1,000 UHR channels

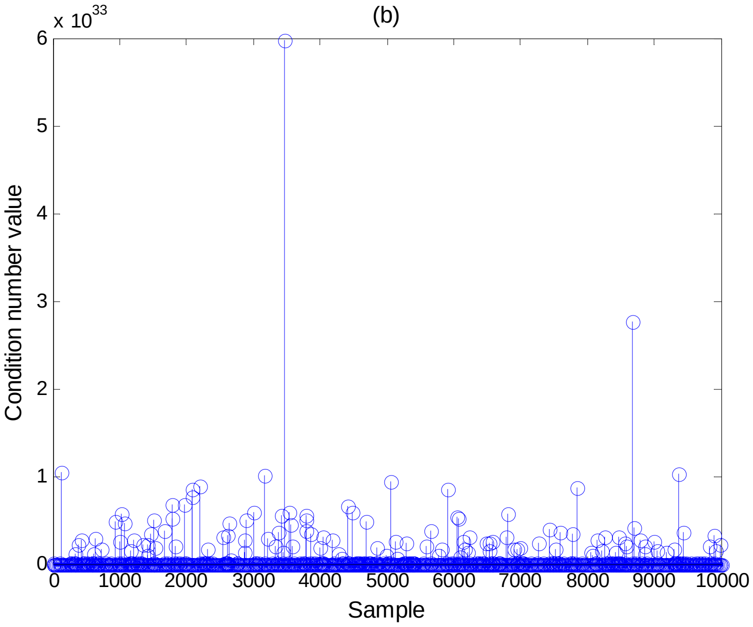

Figure 2.16: Condition number of 1,000 CLR channels

2.5.3 Mode Selection Strategies

Under certain channel conditions, we may want to know which space-time processing technique can perform better. In our implementation, we use the measured throughput to evaluate the performance, since throughput has the advantage of easy calculation. The definition of throughput is as follows:

$$\text{Throughput} = \frac{\text{Successful Bits}}{\text{TransmissionTime}}(\text{b/s})$$

where transmission time is the time used to transmit data part without overheads, and successful bits refer to the successfully received data bits after removal of overheads and process of decoding. Therefore, the major mode selection strategies are based on the throughput performance under different channel conditions.

The selection strategies can be summaries as follows

1. Determine the channel condition by calculating the condition number, and quantized the value to fall into some specific values.
2. According to the channel condition (quantized condition number), we may look up the corresponding table to choose the optimal mode.

The quantization method is simply a bisection method. By choosing the condition number K =10, 20, 30, 40, 50, 100, 200, 400, and 1000 in advance, we can build up the boundaries of interval with K =15, 25, 35, 45, 75, 150, 300, and 700. Therefore, we can quantize the real-time value K to fit the table index. The tables mentioned above are pre-built by imposing different channel conditions with different values of K on the simulated system. More detailed experimental results and performance analysis will be provided in Chapter 4.

2.6 Summary

In this chapter, we first introduce the MIMO-OFDM system, and propose our system architecture including transmitter and receiver. We also give the description of all functional blocks in the order of data passing through a system. At the transmitter, convolutional encoder, interleaver, mapper, adding preamble channel, and frame structure are gone through. At the receiver, synchronization is first mentioned, which consists of coarse timing, fine timing, frequency, and phase synchronizations. Then, channel estimation, de-mapper, de-interleaver, and viterbi decoder are described in the rest part of the receiver. After that, we highlight the space-time coding techniques, also called MIMO techniques, implemented on the system as an independent subsection to give a detailed introduction. Finally, we try to provide a mode selection strategy by first categorizing channel conditions by condition number and then looking up the corresponding tables we build in advance. More detailed experimental results and performance analysis will be given in Chapter 4.